

University of Nebraska - Lincoln
DigitalCommons@University of Nebraska - Lincoln

Civil Engineering Faculty Publications

Civil Engineering

2019

Post-Earthquake Assessment and Numerical Modeling of Freestanding Heritage Structures


M. Khalid Saifullah

University of Nebraska-Lincoln, khalid.saifullah@huskers.unl.edu

Christine E. Wittich

University of Nebraska - Lincoln, cwittich@unl.edu

Follow this and additional works at: <https://digitalcommons.unl.edu/civilengfacpub>

 Part of the [Architectural Engineering Commons](#), [Historic Preservation and Conservation Commons](#), and the [Structural Engineering Commons](#)

Saifullah, M. Khalid and Wittich, Christine E., "Post-Earthquake Assessment and Numerical Modeling of Freestanding Heritage Structures" (2019). *Civil Engineering Faculty Publications*. 155.

<https://digitalcommons.unl.edu/civilengfacpub/155>

This Article is brought to you for free and open access by the Civil Engineering at DigitalCommons@University of Nebraska - Lincoln. It has been accepted for inclusion in Civil Engineering Faculty Publications by an authorized administrator of DigitalCommons@University of Nebraska - Lincoln.



Post-Earthquake Assessment and Numerical Modeling of Freestanding Heritage Structures

M. Khalid Saifullah¹, Christine E. Wittich²

¹Ph.D. Student, Department of Civil Engineering, University of Nebraska - Lincoln, NE, United States.

²Assistant Professor, Department of Civil Engineering, University of Nebraska - Lincoln, NE, United States.

ABSTRACT

Historic and heritage structures are particularly vulnerable to earthquakes, where damage or collapse can not only lead to loss of a structure but also the loss of irreplaceable heritage. Many heritage structures can be classified as freestanding (detached) structures, including unreinforced masonry walls, classical multi-drum columns, and statue-pedestal systems. However, the seismic response of freestanding structures (sliding, rocking, rock-slide, overturning) is poorly predicted by existing methods due to geometric non-linearities as well as sensitivity to interface conditions and modeling parameters. Previous studies have focused on analytical modeling of simplified systems and/or experimentation under controlled laboratory conditions. In contrast, this paper presents the post-earthquake assessment of multiple statue-pedestal systems following the 2014 South Napa earthquake. The objective is to examine the seismic response of these complex freestanding structural systems, under real-world conditions, to elucidate key characteristics of the response and evaluate the influence of both physical and modeling parameters. In this study, the responses of the selected statues from the Napa area are numerically simulated under original ground motion records. The complex geometries of the statues are represented using meshes generated from lidar-based point clouds obtained during post-earthquake reconnaissance. The responses of the statues are simulated using the Distinct Element Method (DEM) where the statue and pedestal have been modeled as rigid blocks with deformation concentrated at the joints (i.e. interface of statue and pedestal or pedestal and ground). The study analyzes the results of the numerical simulations in comparison to the observed physical response during the earthquake event. Results emphasize the significant impact of ground motion parameters (e.g. directionality), the presence of soil, and modeling parameters such as contact stiffness.

Keywords: rocking, freestanding structure, heritage, distinct element modeling, seismic analysis

BACKGROUND AND MOTIVATION

Structures that are unrestrained and free to uplift are termed freestanding structures. These structures are considered particularly vulnerable to earthquakes due to their freestanding nature, which may bring about complete failure of the structure due to overturning instability. These structures may include civil structures such as masonry walls, electrical structures such as transformers, nuclear structures such as gas cooled reactor core, etc. On the other hand, there is wide range of historical structures that fall in the category of freestanding structures including multi-drum columns, unreinforced masonry walls, and statue-pedestal systems which may be a single block or a system of detached structures. Given the historical significance of these structures, it is vital to understand the behavior of these systems for seismic response mitigation.

However, the response of these freestanding structures is poorly predicted as compared to their fixed-base counterparts. This is largely due to the complex dynamics of these systems in which small changes in interface or geometric parameters can lead to large changes in response. Unlike conventional restrained structures, freestanding structures do not possess (classical) natural modes of vibration and their behavior is predominantly governed by rigid body motion. The behavior of even a single block freestanding rigid structure is highly non-linear with respect to the block's geometry as demonstrated by Housner as early as 1963 [1]. The multi-block problem is even more complex due to the ability of the set of blocks to rock, slide or rock-slide (combination) in various rigid body configurations (modes). For example, the response may repeatedly transition from one mode to another during a single ground motion – thus increasing the complexity of the problem [2]. In addition, the dynamic behavior is greatly influenced by small perturbations in geometric, contact, ground motion and numerical parameters. Most of the previous studies focused on simple systems analyzed analytically and/or experimentally under controlled laboratory conditions and largely in a two-dimensional space [2-5]. Three-dimensional analysis, although more complex, presents a realistic scenario for understanding of the problem. Papantonopoulous et al. [6] compared the experimental and numerical response of a multi-drum classical column and concluded that the Distinct Element Method can predict the seismic response of these structures. They also determined that zero damping produced satisfactory results for the strong-motion part of the

freestanding structure's response. Similarly, Psycharis et. al. [7] studied the seismic behavior of part of a historical monument (Parthenon Pronaos in Greece) using the Distinct Element Method and found it as an effective approach for seismic analysis. Peña et al. [8] experimentally studied the rocking dynamics of single rigid-block structures and concluded that repeating an experiment under random ground motions may lead to large changes in response, which indicates the sensitivity of rocking motion to small changes in geometry and initial boundary conditions. Similar findings were determined by Ambraseys and Psycharis [9], who conducted a numerical study on the response of a simplified geometric model of a large statue resting unattached on a multi-drum freestanding column and concluded that these structures are sensitive to small changes and any numerical results on these complex assemblies should be viewed as more qualitative than quantitative. All these studies emphasize the highly nonlinear behavior of freestanding structures.

On the other hand, the studies on the response of asymmetric structures are few and far between. Purvance [10] studied the responses of symmetric and asymmetric blocks to random horizontal vibrations but the focus was on probabilistic relationships for the overturning behavior with application to precariously balanced rocks. Recently, Wittich and Hutchinson [11-12] investigated the response of single and dual-body asymmetric freestanding structures through a series of shake table tests. Their results emphasize the multi-modal behavior of these systems as well as the potential for three-dimensional response even in cases of apparent symmetry. Additionally, their findings further signify the complexity of response in relation to geometric, physical, and ground motion parameters.

This study is an attempt to explicate the behavior of these complex freestanding structures, under real-world conditions, in three-dimensional space. The study employs two statue-pedestal systems which were found overturned following the 2014 South Napa Earthquake during a post-earthquake reconnaissance. Due to the close proximity of ground motion recording stations to the location of these statue-pedestal systems, the earthquake input to these statues is precisely known. The seismic analyses of these systems under their respective ground motions can help elucidate the impact of various physical parameters such as contact stiffness, ground motion directionality, presence of soil at contact interface, and orientation of statue. Since the post-earthquake position of these systems is known, a comparison of the response obtained from numerical analyses and the observed physical response is crucial for understanding of the behavior of these systems. The complex geometries are modeled in a distinct element program using lidar-based geometry and a number of dynamic analyses are conducted.

DESCRIPTION OF STRUCTURES AND EARTHQUAKE EVENTS

The statue-pedestal systems under consideration were located in Napa, California, and were found overturned following the South Napa Earthquake in August 2014. Each of these statues was located in close proximity to a seismic monitoring station providing a known input to the statues. A brief description of these structures and the strong ground motion recordings is provided in this section.

Statue 1 (Justin-Siena High School)

This statue was situated in a garden on the boundary of a courtyard at Justin-Siena High School (Napa, CA). This Marian statue is a sculptured likeness of Our Lady of Guadalupe. The statue and the pedestal are constructed of concrete with the statue having a smaller hexagonal base but a wider central portion. The complex geometry of the statue is mainly concentrated on the front side while the back is relatively flat. The pedestal is a hollow rectangular block with larger areas at the top and the base. The statue-pedestal interface and pedestal-ground interface were unrestrained (in simple contact) thus making this assembly a multi-block freestanding structural system resting on a softer soil-mulch combination in a garden. The statue in its original undisturbed position (prior to the earthquake) was facing west. Following the earthquake, the statue was found overturned towards the east; however, interestingly, the statue rotated approximately 180 degrees about its vertical axis to land in a face-down position. No apparent motion of the pedestal was observed. Throughout this text, this statue-pedestal system is referred to as Statue 1. The positions of the statue-pedestal system before and after the earthquake are shown in Figure 1a and 1b.



Figure 1. Statue 1: a) pre-earthquake, and b) post-earthquake. Statue 2: c) pre-earthquake, and d) post-earthquake. Photos in a and b courtesy of Justin-Siena High School. Photo in c modified from [13]. Photo in d courtesy of Ceja Vineyards.

Statue 2 (Ceja Vineyards)

This statue was situated in a small wine store in downtown Napa. The statue and pedestal are made up of fiberglass reinforced concrete. The statue is a depiction of Bacchus, the Roman god of wine. Similar to Statue 1, the statue-pedestal contact and the pedestal-ground contact are unrestrained; however, the ground in this case is a concrete-flagstone tile floor. The geometry of this statue is more complex as compared to Statue 1. The geometric complexity is fairly concentrated on the front and the sides with a relatively flat portion on the back. The pedestal has a bulged/curved geometry at mid-height. The top and the bottom of the pedestal are flat, with the bottom having a relatively larger area. The long direction of the pedestal was oriented in the east-west direction, and no apparent motion of the pedestal was observed following the earthquake. The statue overturned in the north-east direction during the earthquake – see Figure 1c and 1d. In the subsequent sections of this paper, this statue-pedestal system is identified as Statue 2.

2014 Napa Earthquake

The South Napa (American Canyon) Earthquake ($M_w = 6.0$) struck the San Francisco Bay Area at 3:20 am on August 24, 2014. It was the largest earthquake to strike the Bay Area since the 1989 Loma Prieta Earthquake ($M_w = 6.9$). With the epicenter located just 8 km south-southwest of the city of Napa, the event particularly affected the cities of Napa and Vallejo. Complete collapse of buildings was not observed during this event; however, some older structures incurred serious structural damage. Damage of nonstructural components was by far the most common. With 8 ground motion recording stations in the affected area including 3 in the city of Napa, the ground motion data is well recorded for this event. Given that both statues of interest were located approximately within 270-275 m of respective recording stations, the ground motion data can be conveniently used to investigate the behavior of these structures during that event. The locations of these statues with respect to seismological recording stations is shown in Figure 2 and the strong motion recordings at each station are provided in Figure 3. The peak ground acceleration recorded by the station closest to Statue 1 was 0.43g (EW), and the peak ground acceleration recorded by the station closest to Statue 2 was 0.61g (NS). The time histories of ground acceleration at both sites show noticeable pulses between 3 and 6 seconds, due to the close proximity to the fault. Strong velocity pulses, such as with these ground motions, are known to correlate with overturning of freestanding structures.



Figure 2. Location of statues and ground motion recording stations: a) Statue 1 b) Statue 2.

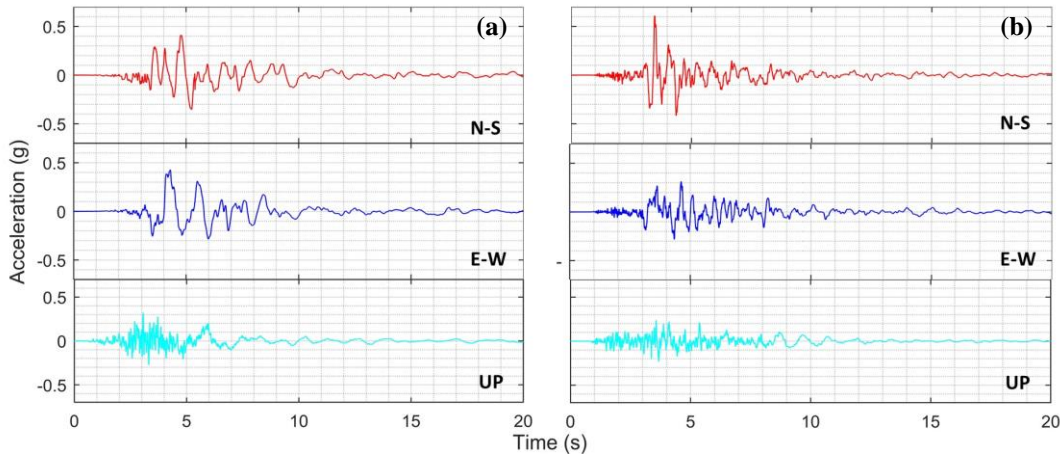


Figure 3. Ground Motion Records: a) Napa Fire Station #3 record b) NCSN Station N016 record.

METHODOLOGY

For the numerical analysis of freestanding structures, the Distinct Element Method (DEM) is preferred over the finite element approach since it can efficiently handle large displacements and rotations; and, therefore, it can provide a more satisfactory representation of failure modes involving the complete detachment of blocks (e.g., statues and pedestals). In DEM, each block is treated as a separate entity and the discontinuities between the blocks are treated as the boundary conditions. 3DEC [14], a numerical analysis software based on DEM approach, is used herein. 3DEC was developed as a result of the fundamental work by Cundall who proposed the distinct element method in the 1970s [15-16]. 3DEC uses an explicit algorithm to solve the equation of motion at each time step and can effectively deal with various geometric interactions.

The statues are modeled in 3DEC using imported mesh geometries while pedestals are modeled directly within 3DEC due to their relatively simple geometry. The complex statue geometry was captured by laser scanning yielding a three-dimensional point cloud during post-earthquake reconnaissance, which was subsequently processed into a three-dimensional surface mesh [17] – see Figure 4. The pedestal of Statue 1 is modeled as a hollow rectangular block which approximates the actual geometry – see Figure 1b and Figure 4a. The pedestal of Statue 2 is modeled as a trapezoidal prism which simplifies the actual geometry shown in Figure 1c and Figure 4b but maintains the surface area at the top and bottom as well as the rocking radius which is a key factor that governs the response. The geometry and the dimensions of these statue-pedestal systems are shown in Figure 4. Since the statues and pedestals are made of concrete or concrete-like material, a mass density of 2400 kg/m^3 is assumed. A rectangular ground block of similar material is introduced at the base of each statue-pedestal system to which ground motion is applied. The ground motion is applied directly to the ground block as a velocity time history. The statues, pedestals, and ground blocks are modeled as rigid blocks with the deformation concentrated only at the statue-pedestal and pedestal-ground interfaces. Since the structures can be considered as an assembly of freestanding blocks, internal elastic deformations of blocks may be neglected and rigid block modeling is an appropriate representation of the physical behavior.

Distinct element codes rely on a point contact approach for the mechanical interaction of blocks in contact. Various types of interactions involving edges, faces, and vertices are checked, and the contact type is determined based on number of touching vertices from each block. In 3DEC, the “common-plane” concept is used to check if two neighboring blocks are actually in contact. If the block face is in contact with the common plane, it is discretized into sub-contacts. The sub-contacts are created at the vertices of the block face by triangulating the faces of blocks. The interface forces, sliding, and separation between the blocks are tracked at these sub-contacts. When the blocks are in contact, the contact representation is equivalent to two sets of springs in parallel with the overall interface behavior taken as the average of both sets. For an accurate stress analysis, an appropriate number of contact points are necessary. Therefore, in this study, to create an adequate number of contacts and sub-contacts, the faces of blocks are split into several smaller facets by splitting and triangulating the block surfaces.

The joint constitutive model is an important parameter which governs the response of rigid block models. The contact/joint constitutive model adopted is Coulomb-Slip Model. The model is based on elastic stiffness, cohesive, tensile and frictional properties and simulates displacement-weakening behavior. For this study, the tensile strength of the joint in the normal direction is considered as zero; therefore, the joint comprised of idealized spring elements is active in compression only. In addition, the contribution of cohesion to the shear strength of the joints is not considered and the shear strength is governed by friction. The parameters used in this study to define the constitutive model for contacts/interfaces are presented in Table 1.

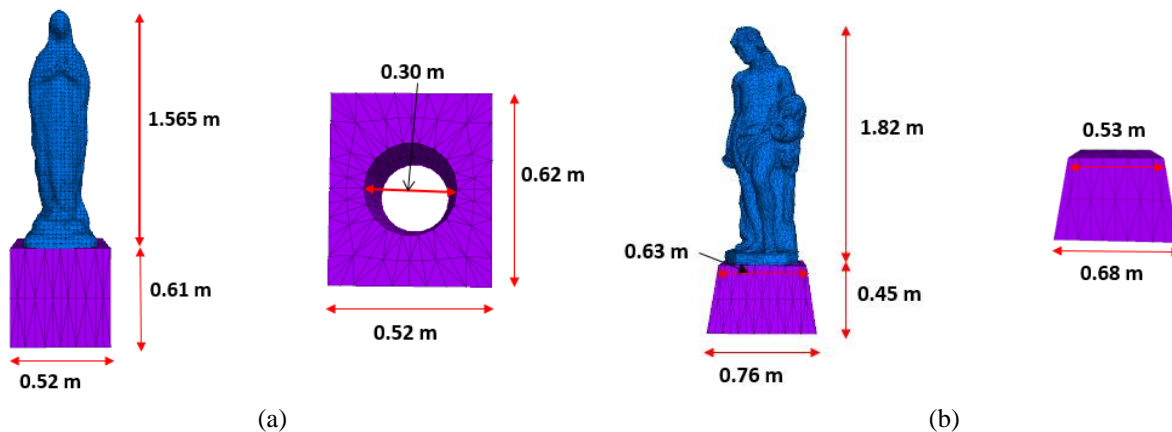


Figure 4. Dimensions of a) Statue 1 and its pedestal b) Statue 2 and its pedestal.

Table 1. Constitutive Model for Contacts

Parameter	Value (or Range)
Normal Stiffness, k_n (GPa/m)	0.1 to 3 GPa/m
Shear Stiffness, k_s (GPa/m)	0.1 to 2 GPa/m
Friction Angle	40°
Cohesion	0 MPa
Tensile Strength	0 MPa

RESULTS AND DISCUSSIONS

The responses obtained from the numerical analysis of both statue-pedestal systems using DEM approach are summarized in this section. Though a large number of analyses are performed, only a few of those cases are presented here for brevity. Statue 1 is subjected to the Napa Fire Station # 3 record, while the response of Statue 2 is studied under the NCSN Station N016 record. Despite the fact that these two statues were geographically close to each other and represent similar types of structural systems, the results of Statue 1 and Statue 2 are presented separately as they possess different geometries and were subjected to different initial conditions during the actual event. The response cases of Statue 1 are employed to study the effect of soil at the ground-pedestal interface – relatively unique condition at its site. At the same time, an attempt is made to study the effectiveness of DEM approach in predicting the actual response of this freestanding structure by comparing the final overturned positions from the numerical response with the actual final position of the statue observed following the South Napa Earthquake. The responses obtained from Statue 2 are used to study the effect of initial orientation on the response by rotating the statue about its vertical axis with respect to its original position. It is important to mention that only the orientation of the statue is treated as a variable while keeping the orientation of pedestal unchanged. For Statue 2, the effect of ground motion directionality is also studied by comparing a uni-directional excitation case with a tri-directional excitation case. The time-history responses presented in this section are the displacement responses of a vertex at the top of the statue and a vertex at the top of the pedestal relative to a vertex at the top of the ground. For clarity, the response time histories presented are truncated to include only the most significant motion.

Effect of soil

In reality, Statue 1 was resting on garden soil with mulch covering (as stated earlier); therefore, it is chosen to study the effect of soil at the ground-pedestal interface concurrently with an evaluation of how closely DEM approach can mimic the actual scenario if similar initial conditions are provided. Initially, a comparative study of hard and soft contact at the ground-pedestal interface is conducted under a uni-directional excitation in the x-direction. For this comparison, the hard contact at ground-pedestal interface is characterized by a high value of 2 GPa/m for normal and shear stiffness (k_n and k_s), while a soft contact (representing soil) is simulated by a much lower stiffness value of 0.2 GPa/m (10 % of stiffness value of hard contact). The statue-pedestal contact is treated as a hard contact with a stiffness value of 2 GPa/m in both of these comparison cases as the concrete statue is resting upon a similar concrete pedestal; therefore, the only variable is the stiffness at the ground-pedestal contact. With a hard contact at the ground-pedestal interface, the only significant motion occurs due to the long period pulse at 4 sec (which can be seen in E-W component of Napa Fire Station # 3 record). However, the displacement of the top of the statue is still very small and nearly negligible as seen in the pictorial representation of the response (Figure 5a). On the other hand, with a soft contact at the ground-pedestal interface, a couple of rocking cycles with significant amplitude are visible (Figure 5b). In the first cycle, the pedestal also rocks with the statue but after that the motion of the statue becomes more dominant and a rock-slide motion of the statue causes it to overturn. A slight rotation of the statue over one of the edges of the pedestal is also observed resulting in the statue falling face up. The overturning of the statue is a result of rocking and sliding, and not purely rocking. It appears that the rotation of the statue over the edge of the pedestal also contributes to instability and overturning of the statue. In both of the cases (i.e. hard contact and soft contact) the pedestal does not overturn; however, its motion becomes more prominent with a soft contact with ground.

Once it is observed that the soft-contact or soil at the statue-pedestal interface can have a significant impact on the motion and stability of the statue when subjected to a uni-directional earthquake input, a more realistic picture of the response is obtained by using a tri-directional input for analyses. Figure 5c presents the results for Statue 1 under the three-dimensional excitation with k_n and k_s values of 0.2 GPa/m for ground-pedestal contact and k_n and k_s values of 2 GPa/m for statue-pedestal contact (as used earlier for uni-directional analyses). For this configuration, the statue rotates by almost 180 degrees followed by overturning resulting in a face-down orientation of the statue (as observed post-earthquake). Only 1 or two cycles of rocking were observed before overturning. During the complex motion, the statue rotates on one of the edges of the pedestal, and overturns face down. While mild rocking and sliding of the pedestal are observed, the pedestal remains stable with only minimal residual displacement. The final position of the statue and the pedestal from the numerical analysis is similar to the post-

earthquake final position of the original statue-pedestal system. It can be argued that the distinct element method possesses the ability to predict the response with sufficient accuracy.

In an effort to briefly study the impact of contact stiffness, the effect of soft soil at the ground-pedestal interface is simulated by using a further lower stiffness value of 0.1 GPa/m for normal stiffness (k_n) and shear stiffness (k_s). A hard-contact at statue-pedestal interface is assumed by using a stiffness value of 1 GPa/m for normal stiffness (k_n) and shear stiffness (k_s) – again 10 times stiffer than the soft contact. The response of the statue and its final position, in general, is similar except that bouncing of the statue off the pedestal is observed prior to overturning (Figure 5d). Therefore, there could be a range of stiffness values or a set of stiffness values that yield realistic results. For the other sets of stiffness values considered in the study, the response of the statue and the final position are quite different if subjected to the same three-dimensional motion. It is noted that the response is largely dictated by the normal and shear stiffness values of both contacts. A small change in stiffness value for any contact, whether normal or shear, can lead to significant change in response.

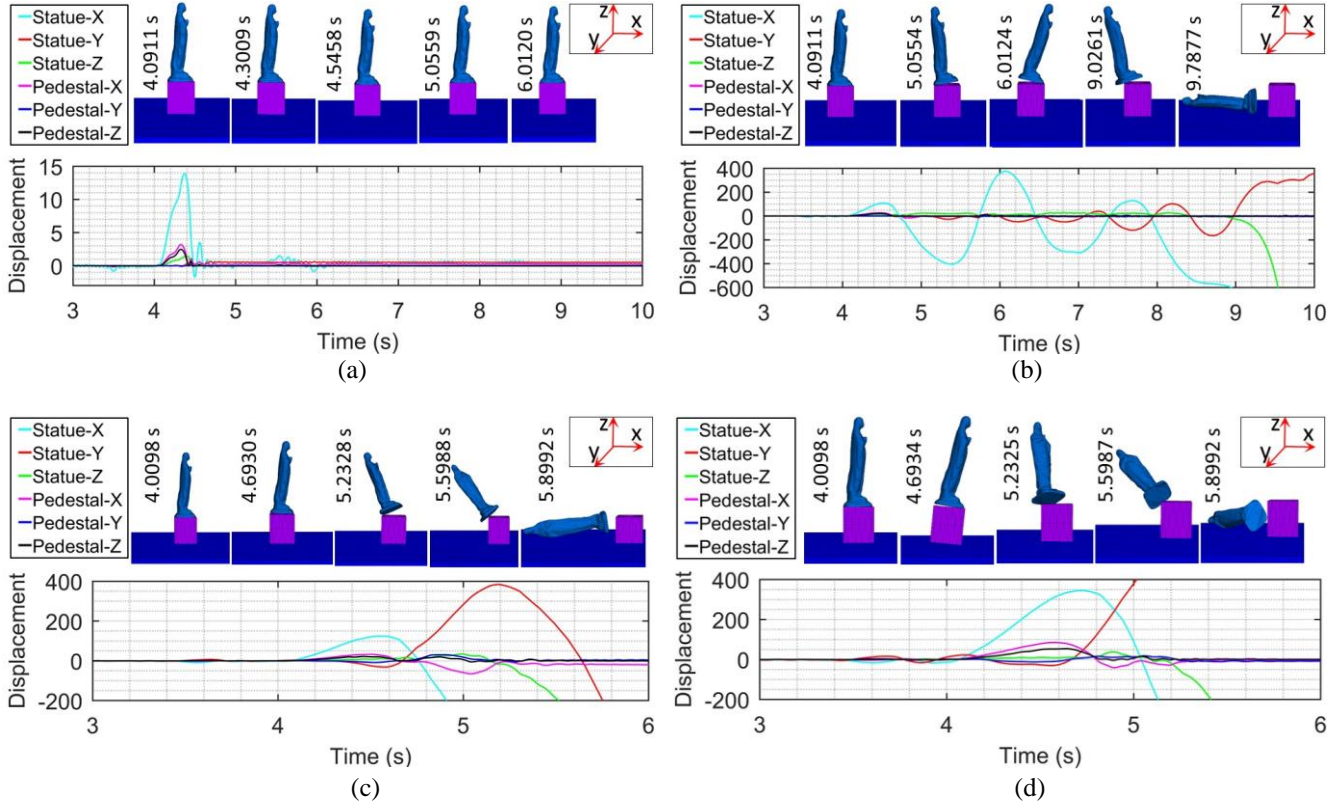


Figure 5. Response of Statue 1 with a) Hard contact (2 GPa/m) at pedestal-ground interface under unidirectional excitation, b) Soft contact (0.2 GPa/m) at pedestal-ground interface under unidirectional excitation, c) Soft contact (0.2 GPa/m) at pedestal-ground interface under tri-directional excitation, and d) Soft contact (0.1 GPa/m) at pedestal-ground interface under tri-directional excitation - (Displacement in mm)

Effect of Initial Orientation

The effect of initial orientation on the response is studied by rotating Statue 2 about its vertical axis through an angle of 27.5 degrees clockwise with respect to original benchmark (unrotated) configuration. The angle is selected so that one of the edges of the footprint of the statue is parallel to the front edge of the top of pedestal. It is also ensured that none of the edges/corners of statue footprint projects off the pedestal. For the original and rotated configurations, stiffness values of $k_n=2$ GPa/m and $k_s=1$ GPa/m are used to define both the pedestal-ground contact and statue-pedestal contact. The behavior of the statues is evaluated under a tri-directional excitation. The response of the statue in both the original configuration and in a rotated configuration results in overturning. The primary difference is with respect to the duration of rocking and the direction of failure. Referring to Figure 6a for the statue with the original orientation, initial minor rocking is observed about multiple edges of the statue's footprint. The multi-edge rocking indicates a certain degree of wobble or twist. Substantial rocking is not observed until approximately 8s. At this point in the statue's response, the rocking is about two opposite edges of the roughly octagonal base. These edges correspond to the most asymmetric and slender cross-section of the statue, which ultimately leads to overturning about this edge. Referring to Figure 6b for the statue in the rotated configuration, similar minor rocking (wobble)

is observed early on in the motion. However, this minor rocking does not have the wobble characteristics of the original configuration. Rather, the motion is initiated about the edges corresponding to the most slender cross-section. Therefore, the statue's response becomes significant much earlier (around 5 – 6s) and overturns closer to 7s. It is noted that the overturning in both cases is about a common edge of the statue – emphasizing the impact of the statue's unique geometry rather than the initial orientation. In another comparison case under a bi-directional input (not presented herein), the statue in rotated and unrotated configurations end up in similar final positions – further emphasizing the impact of the complex geometry.

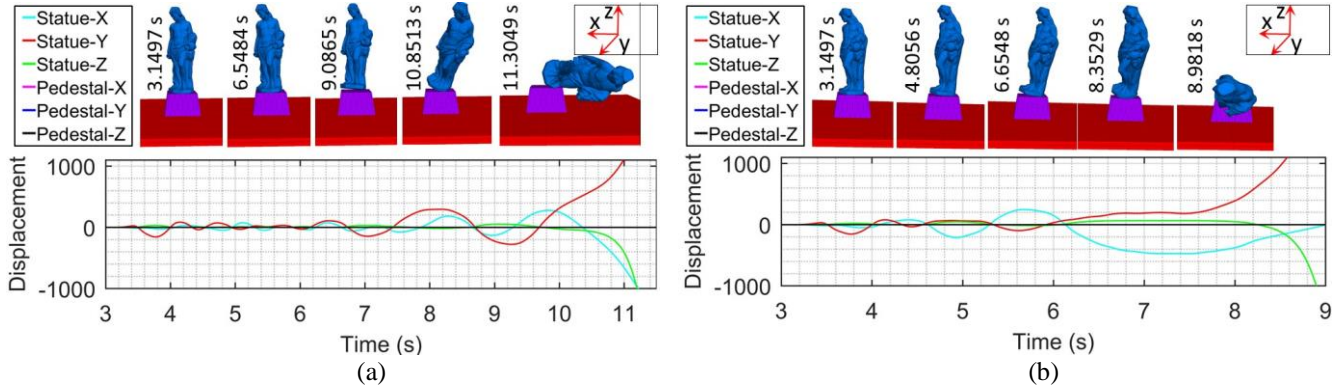


Figure 6. Response of Statue 2 for a) Unrotated configuration b) Rotated configuration - (Displacement in mm).

Effect of ground motion directionality

The effect of ground motion directionality is studied by comparing unidirectional (Y-input excitation) case with a tri-directional input case. The Y-direction is chosen for the unidirectional case since the predominant overturning behavior occurs in this direction. For both the unidirectional and tri-directional cases, the ground-pedestal contact is characterized by $k_n = 2 \text{ GPa/m}$ and $k_s = 2 \text{ GPa/m}$, while the statue-pedestal interface is characterized by $k_n = 1 \text{ GPa/m}$ and $k_s = 1 \text{ GPa/m}$. Under unidirectional input, the statue primarily rocks in Y-direction since the ground motion input is in the Y-direction (Figure 7a). But owing to its asymmetric geometry and the octagonal footprint, rocking in the X-direction is also prominent. The motion also involves some sliding. The flat faces/edges of the statue footprint may be the contributing factor which causes it to overturn over one of its edges at 10 s. Under a tri-directional input, the movement of the statue is observed in both X and Y directions as was observed for unidirectional input in Y-direction (Figure 7b). Until 7 secs, the behavior of the statue under tri-directional input is not so different from the behavior under the unidirectional input. The statue in the case of 3D input overturns earlier than the statue under unidirectional input but they overturn over the same face of the statue footprint. Apart from the ground motion, it looks like the asymmetric geometry and the footprint of the statue are the contributing factors towards similar final position.

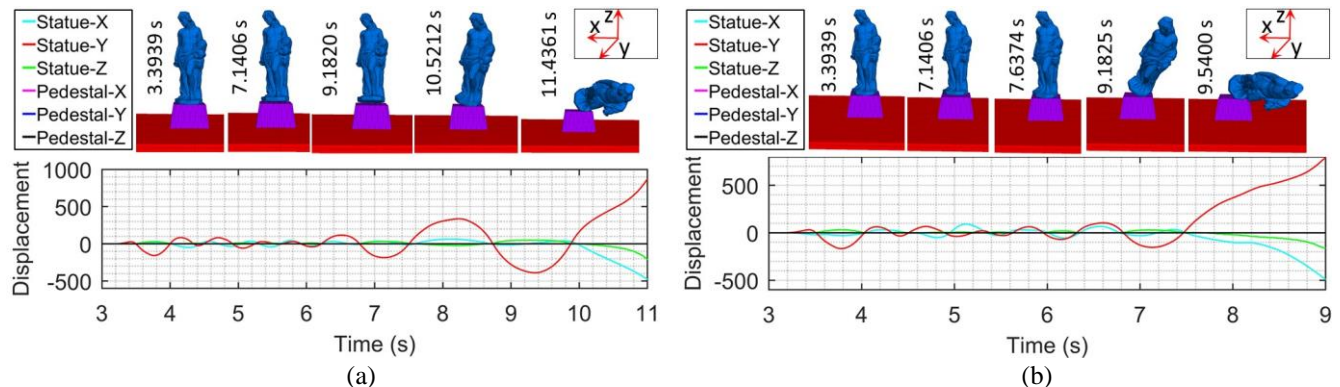


Figure 7. Response of Statue 2 under a) Unidirectional input b) Tri-directional input - (Displacement in mm).

CONCLUSIONS

This paper presents the post-earthquake assessment of two unique statue-pedestal systems following the 2014 South Napa earthquake. The objective is to examine the seismic response of these complex freestanding structural systems, under real-world conditions, to elucidate key characteristics of the response and evaluate the influence of both physical and modeling

parameters. In this study, the complex geometry of the statues was obtained via lidar scanning and the seismic response of the statue-pedestal systems were simulated using the Distinct Element Method. This modeling approach was able to capture the complex three-dimensional response of the statue-pedestal systems well – with the final collapsed positions of the statues corresponding to that observed during post-earthquake reconnaissance. In addition, the incorporation of softer contact stiffnesses at the pedestal-ground interface to reflect soil were able to sufficiently capture the realistic response, where the typical harder contact values failed to do so. Further numerical studies emphasized the significant impact of complex geometry and footprint shape for the freestanding structural response. However, the seismic response is quite sensitive to small changes in the geometry, footprint, and contact parameters. To address this, future work should incorporate probabilistic approaches.

ACKNOWLEDGEMENTS

The authors gratefully acknowledge the University of Nebraska-Lincoln College of Engineering for partial support of this numerical study. The first author was also partially supported by the Layman Foundation of the University of Nebraska-Lincoln. Photographs and documentation regarding the post-earthquake positions and conditions of the two statues were generously shared by Justin-Siena High School (Napa, CA) and Ceja Vineyard (Napa, CA).

REFERENCES

- [1] Housner, G. W. (1963). “The behaviour of inverted pendulum structures during earthquakes,” *Bulletin of the Seismological Society of America*, 53(2), 403–417.
- [2] Psycharis, I. N. (1990) “Dynamic behavior of rocking two-block assemblies,” *Earthquake Engineering and Structural Dynamics* 19, 555–575.
- [3] Allen, R. H., Oppenheim, I. J., Parker, A. R., and Bielak, J. (1986). “On the dynamic response of rigid body assemblies.” *Earthquake Engineering & Structural Dynamics*, 14(6), 861–876.
- [4] Sinopoli, A. (1989) “Dynamic evolution by earthquake excitation of multiblock structures”. In *International Conference on Structural Conservation of Stone Masonry: Diagnosis, Repair and Strengthening*, Hellenic Ministry of Culture, Athens.
- [5] Konstantinidis, D. and Makris, N. (2005). “Seismic response analysis of multidrum classical columns,” *Earthquake Engineering and Structural Dynamics*, 34, 1243–1270.
- [6] Papantonopoulos, C., Psycharis, I. N., Papastamatiou, D. Y., Lemos, J. V., and Mouzakis, H. P. (2002). “Numerical prediction of the earthquake response of classical columns using the distinct element method.” *Earthquake Engineering & Structural Dynamics*, 31(9), 1699–1717.
- [7] Psycharis, I. N., Lemos, J. V., Papastamatiou, D. Y., Zambas, C., and Papantonopoulos, C. (2003). “Numerical study of the seismic behaviour of a part of the Parthenon Pronaos.” *Earthquake Engineering & Structural Dynamics*, 32(13), 2063–2084.
- [8] Peña, F., Prieto, F., Lourenço, P. B., Costa, A. C., and Lemos, J. V. (2007). “On the dynamics of rocking motion of single rigid-block structures.” *Earthquake Engineering & Structural Dynamics*, 36(15), 2383–2399.
- [9] Ambraseys, N., and Psycharis, I. N. (2011). “Earthquake Stability of Columns and Statues.” *Journal of Earthquake Engineering*, 15(5), 685–710.
- [10] Purvance MD. (2005). “Overturning of slender blocks: numerical investigation and application to precariously balanced rocks in southern California.” Ph.D. Dissertation, Department of Geological Sciences, University of Nevada, Reno.
- [11] Wittich, C. E., and Hutchinson, T. C. (2015). “Shake table tests of stiff, unattached, asymmetric structures.” *Earthquake Engineering & Structural Dynamics*, 44(14), 2425–2443.
- [12] Wittich, C.E., and Hutchinson, T.C. (2017). “Shake table tests of unattached, asymmetric, dual-body systems.” *Earthquake Engineering & Structural Dynamics*, 46(9): 1391-1410.
- [13] Jones, T. J. (2013). “Bach to Bacchus.” Ceja Vineyards, <<http://bachtobacchus.blogspot.com/2013/07/ceja-vineyards.html>> (Dec. 10, 2018).
- [14] Itasca Consulting Group. 3DEC – Universal Distinct Element Code. Minneapolis, U.S.A., 1998.
- [15] Cundall PA. (1988) “Formulation of a three-dimensional distinct element model – Part I: A scheme to detect and represent contacts in a system composed of many polyhedral blocks”. *International Journal of Rock Mechanics and Mining Sciences*, 25,107–116.
- [16] Hart RD, Cundall PA, Lemos JV. (1988) “Formulation of a three-dimensional distinct element model – Part II: Mechanical calculations”. *International Journal of Rock Mechanics and Mining Sciences*, 25,117–125.
- [17] Wittich, C.E., Hutchinson, T.C., Lo, E., Meyer, D., and Kuester, F. (2014). *The South Napa Earthquake of August 24, 2014: Drone-based Aerial and Ground-based LiDAR Imaging Survey*. Structure Systems Research Project Report Series, SSRP 14/09, Department of Structural Engineering, University of California, San Diego, La Jolla, CA